

Utilization of Global Navigation Satellite Systems as non-cooperative transmitters in bistatic radar

M. Cherniakov
University of Birmingham, B15 2TT Birmingham, UK

Abstract

Over recent years, there has been an increasing interest in Global Navigation Satellites Systems (GNSS) as an emitter of electromagnetic energy. Being reflected from objects, these signals carry a lot of information for further analysis. The signals can be received and processed in various ways to extract information about the objects. Methods used include direct reflection, interferometric measurements, as well as imaging via aperture synthesis. Using radar terminology : the transmitter (GNSS satellite) and the receiver form Bistatic Radar (BR) with a non-cooperative transmitter (NCT). This paper is dedicated to selective problems of BR with GNSS as NCT.

Keywords: Bistatic Radar; Non-cooperative transmitter; Global Navigation Satellites Systems; Power budget; System interferences

Introduction

In this paper we will consider bistatic radars which use GNSS as a non-cooperative transmitter [1]. The receiver can be stationary, positioned on a surface or on aerial platforms [2]. The remote sensing research community was the first to propose using specular reflections in such systems for land and oceans monitoring, as well as for meteorological purposes. On the day of preparing this paper, about 170 papers were identified as being dedicated to the problem of GPS signals reflection for remote sensing applications. However, only a few works were dedicated to the radar aspects of the signal's reception and processing. Selected problems of BR with GNSS as NCT are considered in this paper.

Currently only GPS GNSS is in a fully operational state; as well as GLONASS having 12 active satellites [3], the Galileo system is on its way to space [4] and China has advertised their plans for satellite navigations. In some instances, all these systems operate in a similar way and occupy the same frequencies as well as

introducing a similar power density near the surface.

The basic configuration of this radar is shown in Fig. 1.

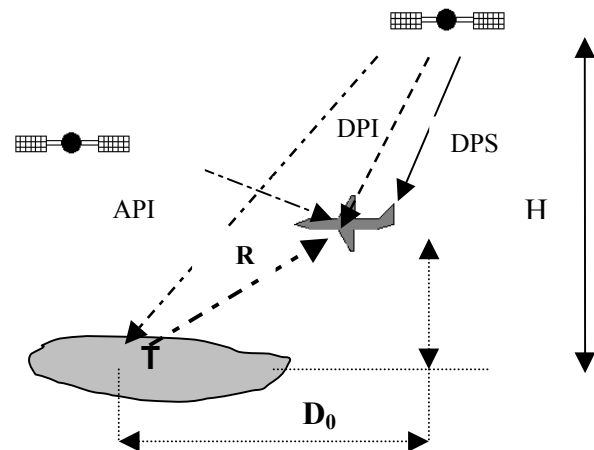


Figure 1: BR with GNSS as NCT
RS-reflected signal; DPS-direct path signal;
DPI-direct and API-adjacent path
interference

The motion of the transmitter or receiver (or both) can be used for the antenna aperture synthesis to provide high spatial resolution (small resolution cell size). This

system can be classified as Bistatic Synthetic Aperture Radar (BSAR) with GNSS NCT. We will use the term ‘Space-Surface Bistatic SAR’ (SS-BSAR with NCT) for this class of systems, assuming an essential asymmetry in the system architecture [5].

There are a number of reasons for the increasing attention given to BR with GNSS NCT. This is based on the unique possibilities of this technology:

- Simultaneous analysis of bistatic and multistatic reflections obtained at different bistatic angles
- Passive operational mode which does not introduce interferences or requires special frequencies allocation
- Extremely high signal stability and simple synchronization
- Light weight, portable size and low cost of the receiving system which can be made from off the shelf components

Of course, these bistatic radars are not aiming to replace all existing radar systems, but will bring essentially new capabilities and find their own niche for various applications [8].

Power budget consideration

One of the key problems of any radar is the power budget, which should be strong enough to provide targets detection. On a practical level, it is expected that BR with GNSS NCT must have a very tough power budget. But we will show that it is strong enough for a number of applications.

Let’s first evaluate this budget for SS-BSAR following the [6, chapter 15] signal to noise ratio (S/N) evaluation and [7] for the detection probability (D) and false alarm (F) estimation. The difference in comparison with this [6],[7] methodic is that we are replacing the calculation of power density near the targets by the known value of this density Π_1 which is specified

for GNSS systems. So, for stationary targets, where coherent integration is assumed to be over all integration time:

$$S/N = \frac{P_t G_t A_r \sigma}{(4\pi)^2 R^4 K T_0 \beta F_n} \frac{\tau_i}{\tau_0} \frac{PRF \cdot R \cdot \lambda}{2V \Delta_{az}} \quad (1)$$

where $P_t G_t / 4\pi H^2 = \Pi_1 \approx 2.2 \cdot 10^{-13} W/m^2$ for GPS and Galileo cases when Glonass generates 3 dB more power density. Omitting some details of the calculations, this equation can be rewritten for our case as follows:

$$\frac{S}{N} = \frac{\Pi_1 A \sigma \lambda \eta}{4\pi R N_n K T_0 V \Delta_{az}} \quad (2)$$

where $\Delta_{az} = \lambda R / L_c$ is the potential azimuth resolution in linear units; $\lambda = 0.19 m$ is the wavelength, L_c is a length of the synthetic aperture, R is the distance from the aircraft (receiver) to the target; V is the aircraft speed; $T_0 N_n$ is the noise temperature; A is the antenna effective area and η is the hardware loss coefficient. Let us assume now that the geometric aperture of the aircraft antenna is $S = 1m \cdot 0.5m$ (1 m along the fuselage) with the efficiency $k_a = 0.7$, as a result we can write in (2) that $A = 0.35$, $\eta = 0.5$, $N_n = 1 dB$. For $\Delta f_c = 10 MHz$, the range resolution is $\sim 15 m$ and the potential (a problem requiring further study) cross range resolution is 1 m. Table 1 shows collected targets detection parameters for a number of typical RCS and aircraft flight parameters.

SS-BSAR power budget Table 1

RCS m^2	R km	V m/s	T_{int} s	S/N dB	D vs F
10	3	50	12	12.5	$0.9 \cdot 10^{-5}$
10	10	50	36	7.3	$0.65 \cdot 10^{-2}$
50	10	50	36	14.3	$0.95 \cdot 10^{-7}$
50	30	50	108	9.5	$0.9 \cdot 10^{-2}$
50	10	100	18	11.2	$0.9 \cdot 0.5 \cdot 10^{-3}$
250	30	50	108	16.5	$0.99 \cdot 10^{-10}$
250	15	100	27	16.5	$0.99 \cdot 10^{-10}$
250	30	100	54	13.5	$0.95 \cdot 10^{-4}$
250	30	150	36	11.7	$0.9 \cdot 10^{-4}$
250	30	200	27	10.4	$0.9 \cdot 2 \cdot 10^{-3}$

Figures from the table clearly indicate that in spite of the limited power budget, a lot of typical ground targets (50 m² for a small vehicle, 250 m² for a tank or a track RCS [6]) could be effectively detected.

System's interferences reduction

An important feature of the system is that reflected signals are always received against a background of direct and adjacent path interferences (DPI and API) (see Fig. 1). These are signals transmitted by satellites and received directly by the radar antenna. Analysis of these interferences in the first approximation was done in [5]. More accurate study of these interferences is a separate subject. Nevertheless, we can predict that at least one of the interferences can be strong enough to mask the reflected signal. In this case a modified version of a sidelobe canceller (SC) [6] can be used.

The typical approaches in radar SC are based on the assumption that interferences are not only essentially stronger than the desired signal but are also above the

thermal noise floor at the receiver output. For the DPI and the API this is not true and they are essentially under the noise, but are dramatically stronger than the reflected signals. So, to tune the array weight coefficients, or in other words to provide adaptation, a filter (correlators – Corr) matched to the interference should be used (Fig.2).

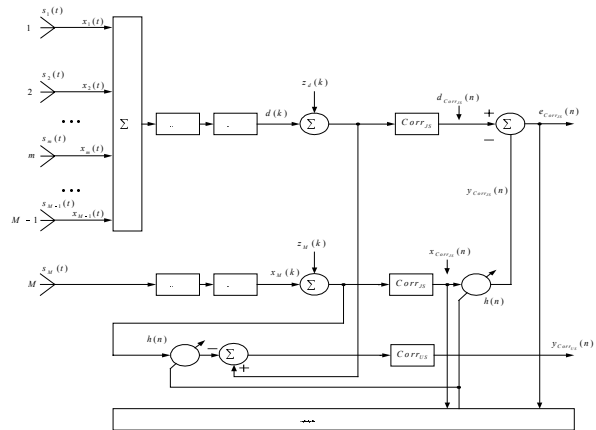


Figure 2: Architecture of the modified canceller

This type of sidelobe cancellers has not been introduced and studied before. Elements #1...(M-1) form the radar antenna and M-th is a tuneable element of the two-channels adaptive SC. RF is the radiofrequency part of a receiver; DC is the base band down converter; $s(t)$ is the input signal; $x_m(t)$ is a continuous signal in m -th antenna; $x_M(k)$ is M -th channel signal; $d(k)$ is the output signal of the main array; $e(k)$ is the output signal of the total array; $h(k)$ is the adaptively adjusted weight, $z_d(k)$ is the noise of the radar receiver, $z_M(k)$ is the noise in the M -th channel. $Corr_{JS}$ is the complex correlator (CC) for the interference evaluation; $d_{Corr_{JS}}(n)$ is the output radar channel signal after processing in CC; $x_{Corr_{JS}}(n)$ is the output signal of M -th element after processing in CC; $y_{Corr_{JS}}(n)$ is the weighted signal $x_{Corr_{JS}}(n)$; $Corr_{US}$ is CC for useful signal evaluation;

$y_{Corr_{US}}(n)$ is the desired signal correlator output; n means sampling at $N_{MS}T_s$ intervals; N_{MS} is M-sequence length (number of chips) and $T_s = 1/f_s$ is the sampling interval.

The modelling results for the noiseless case is shown in Fig. 3-a, where the interference is coming from direction of 50° relevant to the main antenna (M=5) beam access. The same segment is zoomed in for the case of -20 jammer (interference) noise ratio (JNR) and 50 000 chips integration – Fig. 3-b.

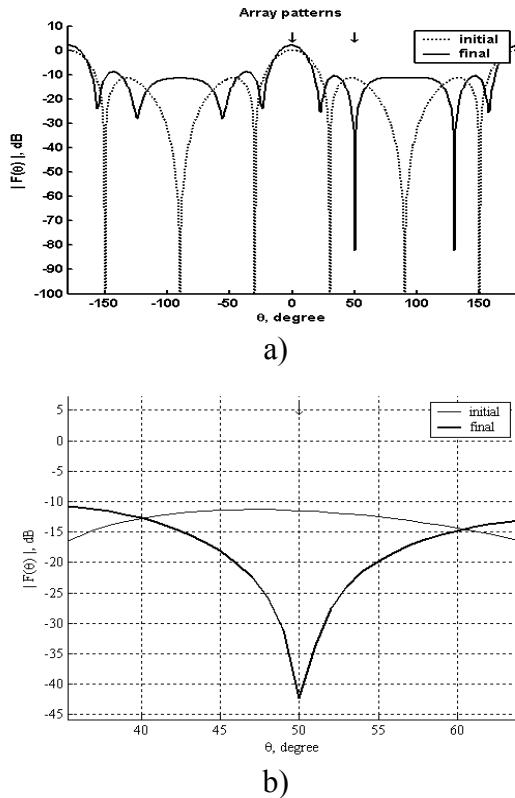


Figure: 3 Interference reduction

Sidelobe canceller performance

In this modified version of the SC two parameters affect the depth of interference suppression: JNR ratio and a delay in adaptation which introduces some sort of a dynamic error (DE). The physical nature of this error is such that during the signal processing, mainly integration time, the direction to the interference can be shifted

and the null of the antenna pattern is then not pointing exactly in the interference direction. So, the integration time itself reduces the noise error, which potentially enforces the DE.

To minimise an integration time we are currently considering adaptive correlators (AC). AC differs from traditional correlators with the reset (RC) with the output signal:

$$d_{Corr_{JS}}(k) = \sum_{i=0}^{N_{MS}-1} X(i)d(k-i) \quad (3)$$

where N_{MS} is the length of the used signal (interference) code $X(i)$. For further adaptive signal processing only the correlator output, accumulated during N_{MS} samples are used. After each N_{MS} samples, the sum in (3) is set to zero value. In contrast AC accumulates this sum continuously as:

$$d_{Corr_{JS}}(n) = \frac{d_{Corr_{JS}}(n-1) + d_{Corr_{JS}}(N_{MS})}{n} \quad (4)$$

where $d_{Corr_{JS}}(N_{MS})$ means the value of (3) after the accumulation of N_{MS} samples. So, its integration time is increased every N_{MS} samples. In Fig. 4 the AC and RC effectiveness is compared.

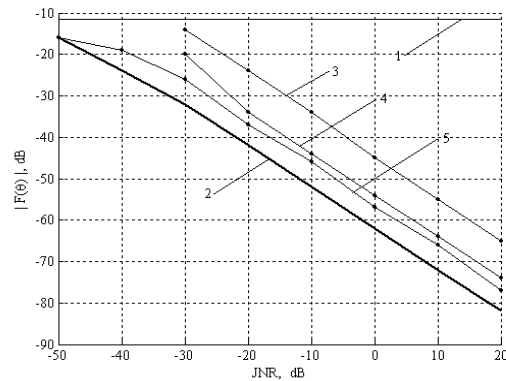


Figure 4: AC and RC for different JNR

The null depth is shown in this figure for 50000 chips integration for different conditions: 1-without adaptation; 2- AC; 3 to 5 RC with the reset time 1023, 2046, 3069 respectively. The longer integration under other equal conditions, the bigger can be the DE. Of course this error depends on the aircraft dynamics.

Positions of the nulls are shown in Fig. 5 after an appropriate integration in an absence of a relative motion between the interference source and the receiver (solid lines), and in the case of 10^0 per second angle speed (dotted lines).

Fig 5-a corresponds to 20 dB and Fig. 5-b is for -20 dB input JIR. As one can see in the first case, the main error is the DE. For the high noise level the null depth has already been restricted by the noise.

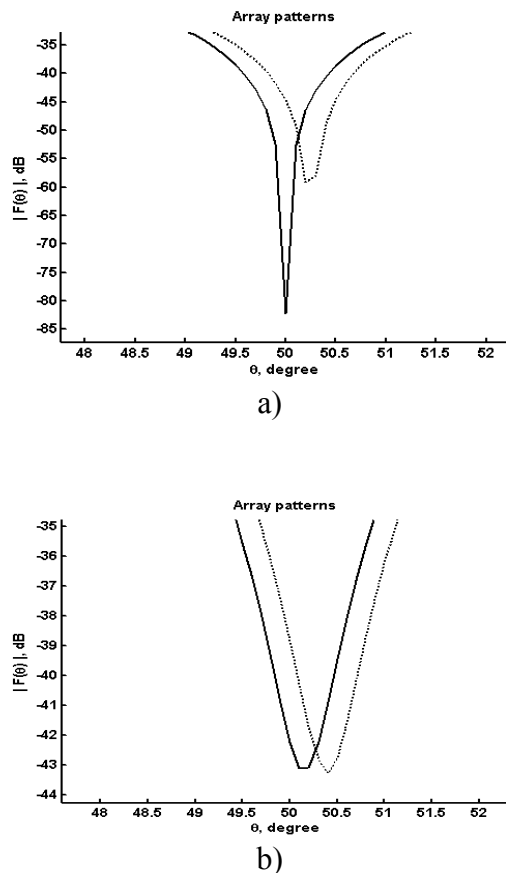


Figure 5: Noise and dynamic errors examples in the adaptive SC

Conclusions

BR with GNSS NCT is the new subclass of radar with a lot of unknown peculiarities. This paper has introduced the system power budget analysis and some problem of adaptive interference protection. In spite of the optimistic results these problems require further in depth study.

References

1. Cherniakov M., Kubik K., *Secondary application of wireless technology*, European Conference on Wireless Technology, Paris, France, October 2-6, 2000, pp. 305 – 309.
2. Cherniakov M., Zeng Tao, Plakidis E., *Ambiguity Function for Bistatic SAR and its Application in SS-BSAR Performance Analysis*, International conference RADAR-2003, Adelaide, Australia, September 2003.
3. <http://www.glonass-center.ru/>
4. <http://www.esa.int/export/esaNA/index.html>
5. Cherniakov M., *Space-Surface bistatic synthetic aperture radar –Prospective and problems*, Radar 2002, 15-17. October 2002, Edinburgh, UK, pp. 22-26
6. Skolnik M., *Radar Handbook*, McGraw Hill, 1990.
7. Barton D., *Simple procedures for radar detection calculations*, IEEE Trans. on Aerospace and Electronic Systems, Sept. 1969, **AES-5**, (9) pp. 837-846
8. Keydel W., *Perspectives and visions for future SAR systems*, IEE Proc.-Radar, Sonar and Navigation, V. 150, No. 3, 2003, pp.97-103